QUARTERLY OF APPLIED MATHEMATICS

Vol. III JANUARY, 1946 No. 4

ON THE STABILITY OF TWO-DIMENSIONAL PARALLEL FLOWS

PART III.—STABILITY IN A VISCOUS FLUID*

BY

C. C. LIN**

Guggenheim Laboratory, California Institute of Technology

11. General considerations. The investigations in Part II* of the stability characteristics of a parallel flow in an inviscid fluid led to very useful information. In the first place, they enable us to visualize the effect of pressure forces very clearly. In the second place, the results can be used as a guide for studying the stability problem in a real fluid, since instability is expected to occur only for sufficiently large Reynolds numbers. Thus, if we know the general characteristics of "inviscid stability" for a given velocity distribution, some stability characteristics in a real fluid can be obtained by considering a *modification* of these results by the effect of viscosity. Such a consideration was first made by Heisenberg, [14]† who demonstrated that the effect of viscosity is generally *destabilizing* at very large Reynolds numbers. There are, however, a few points to be supplemented in his discussion. We shall therefore study this problem in some detail in §12.

To get a good understanding of the stability problem, we want to know the following points for any given *class* of velocity distribution. First of all, we want to know whether this class of flows is stable for *all* Reynolds numbers. Secondly, if it is stable for certain Reynolds numbers with respect to disturbances of certain wavelengths, but unstable under other conditions, we want to know the general nature of the curve $c_i(\alpha, R)=0$ which separates regions of stability and instability in the α, R plane. Thirdly, such a curve will be expected to show a minimum in R, below which all small disturbances are damped out. It is therefore desirable to be able to calculate this minimum critical Reynolds number rapidly.

In the next section, we shall solve these problems for two classes of flows; namely, (a) velocity distributions of the symmetrical type, and (b) velocity distributions of the boundary-layer type. Indeed, it will be shown that *in these cases the flow is always unstable for sufficiently large Reynolds numbers*, whether the velocity curve has a point of inflection or not. The curve of neutral stability $c_i(\alpha, R)=0$ will be shown to belong to either of the types shown in Fig. 9. When the velocity curve has no point of inflection, the two asymptotic branches of the curve have the common asymptote $\alpha=0$

* Received July 18, 1945. Parts I and II of this paper appeared in this Quarterly **3**, 117–142, and 218–234 (1945).

** Now at Brown University.

† The figures in brackets refer to titles in the Bibliography at the end of Part I.

(Fig. 9a). When there is a point of inflection, one branch has the asymptote $\alpha=0$, while the other has the asymptote $\alpha=\alpha_s>0$ (Fig. 9b). In either case, it will be shown that the region inside the loop is the region of instability. It should be observed how these results fit in with those of Rayleigh and Tollmien for the inviscid case, and with the destabilizing effect of viscosity noted by Heisenberg for large Reynolds numbers. Simple formulae will be derived to express the asymptotic branches of the curves in Fig. 9. In fact, it is by means of these asymptotic behaviours and a criterion of stability of Synge [63], that the results mentioned above are established. Simple rules will also be given, by which the minimum critical Reynolds number can be very easily obtained from quantities involving very simple integral and differential expressions of the velocity distribution $w(y)$. Very little numerical labor is involved for the calculation in any particular case.

Heisenberg also discussed the general shape of the curve $c_i(\alpha, R)=0$. However, his argument does not appear to be very decisive, and some of his results are not well stated. He did not obtain the asymptotic forms of the $\alpha(R)$ curve as given below. He also tried to estimate the order of magnitude of the critical Reynolds number, but did not try to make an approximate calculation in terms of simple differential and integral expressions of $w(y)$ (loc. cit., p. 600).

In order to obtain definite numerical results, which may be subjected to experimental verification, we shall apply our theory to the stability problem of special velocity distributions. In §13, we shall give the results of calculation of the neutral curves in (a) the Blasius case and (b) the Poiseuille case. The method of calculation and its numerical accuracy will be given in the Appendix. Frequent reference to the equations in it will therefore be made in the following sections.

12. Heisenberg's criterion and the general characteristics of the curve of neutral stability. We shall now proceed to study the general stability characteristics in a viscous fluid as indicated above. In the first place, we shall develop Heisenberg's criterion in a slightly improved form. We shall then restrict ourselves to velocity distributions of the symmetrical type and of the boundary-layer type. For these cases, we shall prove the results summarized in the next section

a) *Heisenberg's criterion.* Along the neutral curve

$$c_i(\alpha, R) = 0$$

(if it exists), all the parameters α, c, and R are functions of one of them, say, R. Let us restrict ourselves to cases where α and c do not approach zero along the neutral curve as R becomes infinite. Then, the approximations (6.27) are valid for sufficiently large values of R. By using (6.26), (6.24) and (6.27), we can transform (6.13) into the following:

$$\sum_{n=0}^{\infty}\alpha^{2n}K_{2n+1}(c) = \frac{e^{-\pi i/4}}{\sqrt{(\alpha R(1-c)^5}}\left\{\sum_{n=0}^{\infty}\alpha^{2n}K_{2n}(c) + w_2'(1-c)\sum_{n=0}^{\infty}\alpha^{2n}K_{2n+1}(c)\right\}$$
$$+\frac{e^{\pi i/4}}{\sqrt{(\alpha Rc)^5}}\left\{\sum_{n=0}^{\infty}\alpha^{2n}H_{2n}(c) + w_1 c\sum_{n=0}^{\infty}\alpha^{2n}K_{2n+1}(c)\right\}.$$

If there is an inviscid neutral disturbance with $c=c_s$, $\alpha=\alpha_s$, we have

$$\sum_{n=0}^{\infty}\alpha_s^{2n}K_{2n+1}(c_s) = 0.$$

Hence, when $\alpha=\alpha_s$, and $c=c_s+\Delta c$, differing but slightly from c_s, we have

$$\Delta c = \frac{e^{-\pi i/4}}{\sqrt{\alpha_s R(1-c_s)^5}} \frac{\sum_{n=0}^{\infty} \alpha_s^{2n} K_{2n}(c_s)}{\sum_{n=0}^{\infty} \alpha_s^{2n} K'_{2n+1}(c_s)} + \frac{e^{\pi i/4}}{\sqrt{\alpha_s R c_s^5}} \frac{\sum_{n=0}^{\infty} \alpha_s^{2n} H_{2n}(c_s)}{\sum_{n=0}^{\infty} \alpha_s^{2n} K'_{2n+1}(c_s)}. \tag{12.1}$$

Similar considerations of (6.14), (6.15), and (6.17) give respectively

$$\Delta c = \frac{e^{\pi i/4}}{\sqrt{\alpha_s R c_s^5}} \frac{\sum_{n=0}^{\infty} \alpha_s^{2n} H_{2n+1}(c_s)}{\sum_{n=0}^{\infty} \alpha_s^{2n} K'_{2n+2}(c_s)}, \tag{12.2}$$

$$\Delta c = \frac{e^{\pi i/4}}{\sqrt{\alpha_s R c_s^5}} \frac{\sum_{n=0}^{\infty} \alpha_s^{2n} H_{2n}(c_s)}{\sum_{n=0}^{\infty} \alpha_s^{2n} K'_{2n+1}(c_s)}, \tag{12.3}$$

$$\Delta c = \frac{e^{\pi i/4}}{\sqrt{\alpha_s R c_s^5}} \frac{\sum_{n=1}^{\infty} \alpha_s^{2n} H_{2n-1}(c_s) + (1-c_s)^2 \sum_{n=0}^{\infty} \alpha_s^{2n+1} H_{2n}(c_s)}{\sum_{n=1}^{\infty} \alpha_s^{2n} K'_{2n}(c_s) + (1-c_s)^2 \sum_{n=0}^{\infty} \alpha_s^{2n+1} K'_{2n+1}(c_s)}. \tag{12.4}$$

In general, it is not very easy to determine whether $\Delta c_i>0$ or <0. However, when c_s and α_s are both small, but not zero, all the above equations will reduce to

$$\Delta c = e^{\pi i/4}/\sqrt{\alpha_s R c_s^5}\, K_1'(c_s), \tag{12.5}$$

after we make use of the reductions corresponding to (1) and (2) of the Appendix. Now, when c is small,

$$K_1(c) = \int_{y_1}^{y_2} dy(w-c)^{-2} = -\frac{1}{w_1' c} - \frac{w_0''}{w_1'^3}(\log c + i\pi) + O(1);$$

hence, it can be easily verified that $K_1'(c)$ is approximately real and positive for small real values of c. Hence, (12.5) shows that $\Delta c_i>0$ in every case. The disturbance with wave length $2\pi/\alpha_s$, neutrally stable in the inviscid case, is unstable when viscous forces are considered. This result was first obtained by Heisenberg, and may be formulated as follows:

HEISENBERG'S CRITERION. *If a velocity profile has an "inviscid" neutral disturbance with non-vanishing wave number and phase velocity, the disturbance with the same wave number is unstable in the real fluid when the Reynolds number is sufficiently large.*

In Heisenberg's original discussion, only the first type of motion is considered. The last equation on p. 597 of his paper is essentially our equation (12.1) with all the terms in α^2 dropped. Evidently, the above arguments hold only for α_s, $c_s\neq 0$. It will be seen later from Fig. 9 that one neutral disturbance with $\alpha=0$ and $c=0$ for infinite R, is actually stable for finite values of R.

b) *Asymptotic behavior of the neutral $\alpha(R)$ curve.* We shall now study the general asymptotic behavior of the neutral curve, assuming that it exists. The answer to the existence problem will be evident during the course of the investigation. For large values of αR, we would generally expect z of (6.28) to be much greater than 1, but it is also possible for z to approach a finite value or zero. We shall therefore discuss both possibilities.

For large values of z, we have approximately,

$$\mathcal{J}_r = 1, \qquad \mathcal{J}_i = 1/\sqrt{2z^3} = w_1'/\sqrt{2\alpha R c^3}, \tag{12.6}$$

where $\mathcal{J}_i$ is small. If we refer to (5) and (7) of Appendix, we see that the imaginary part v of the right-hand side member of those equations depends on that of $w_1' cK_1(c)$ and those of the integrals H_1, H_2, M's and N's. If α and c are small, which will be verified *a posteriori*, we have only the contribution from the first term; thus,*

$$v = -\pi w_1 \frac{ww''}{w'^3} \quad \text{for} \quad w = c. \tag{12.7}$$

By using (12.6) and (12.7), we see that the equations (8) in the Appendix can be approximated by

$$u = 1, \tag{12.8}$$

and

$$v = -\frac{\pi}{w_1'} cw_0 = w_1'/\sqrt{2\alpha R c^3}. \tag{12.9}$$

These are the equations for determining a relation $\alpha(R)$, if we eliminate c between them.

In the case where $\alpha R c^3$ approaches a finite limit as $\alpha R \to \infty$, c must approach zero. Hence, v must approach zero, and from (8) of Appendix, $\mathcal{J}_i$ must also approach zero. From the curve for $\mathcal{J}_i(z)$, we see that this happens for $z = 2.294$, for which $\mathcal{J}_r = 2.292$. Then, using (9) of Appendix, (12.6), and (12.7), we have

$$\alpha R = w_1'^2 z^3/c^3, \qquad z \doteq 2.294, \tag{12.10}$$

and

$$u = \mathcal{J}_r = 2.292. \tag{12.11}$$

The two types of relations (12.8), (12.9) and (12.10), (12.11) evidently correspond to two different branches of the $\alpha(R)$ curve (cf. Fig. 9). These conditions can be satisfied in cases (2a) and (3) of section 6 (cf. (11.5), (11.7) of Appendix), but it appears to be difficult in case (2b) (cf. (11.6) of Appendix).

CASE (2a). *Symmetrical velocity distribution with symmetrical $\phi(y)$.* We consider the cases where both α and c are small. By using (12.5) and noting that u takes on a finite value in either (12.8) or (12.11), we see that we must have

$$u = \frac{w_1' c}{H_{10}\alpha^2}, \quad \text{where} \quad H_{10} = H_1(0) = \int_{y_1}^{y_2} w^2 dy; \tag{12.12}$$

* In fact, the other terms never give considerable contributions to the imaginary part even for only moderately small values of α and c. This point will be discussed in the Appendix. The approximation (12.7) will be used for all later calculations.

i.e., c must approach zero as fast as α^2. The asymptotic behavior of the $\alpha(R)$ curves as given by (12.8)–(12.11) are as follows:

$$R = (w_1'^{11}/2\pi^2 H_{10}^5 w_0''^2)\alpha^{-11}, \qquad c = (H_{10}/w_1')\alpha^2, \quad \text{(first branch)}, \tag{12.13}$$

$$R = w_1'^5(z/\mathfrak{J}_r H_{10})^3\alpha^{-7}, \qquad c = (H_{10}\mathfrak{J}_r/w_1')\alpha^2, \quad \text{(second branch)}, \tag{12.14}$$

where $\mathfrak{J}_r = 2.292$, $z = 2.294$ approximately.

CASE (3). *Boundary-layer profile.* Here, the equation corresponding to (12.12) is (cf. (7) of Appendix)

$$u = w_1 c/\alpha, \tag{12.15}$$

i.e., c must approach zero as fast as α. Note that in the previous case, the relation (12.12) depends both on w_1' and on $\int_{y_1}^{y_2} w^2 dy$. Here, it depends only on the initial slope of the velocity curve w_1'. The two branches of the $\alpha(R)$ curve for large values of R are

$$R = (w_1'^{11}/2\pi^2 w_0''^2)\alpha^{-6}, \qquad c = \alpha/w_1', \qquad \text{(first branch)}, \tag{12.16}$$

and

$$R = w_1'(z/\mathfrak{J}_r)^3\alpha^{-4}, \qquad c = \alpha\mathfrak{J}_r/w_1' \qquad \text{(second branch)}, \tag{12.17}$$

where $\mathfrak{J}_r = 2.292$, $z = 2.294$ approximately.

Effect of varying curvature in the curve of velocity distribution. In either case, the second branch of our asymptotic curve depends very little upon the shape of the velocity profile, while the first branch depends very much upon it through the term w_0''. This fact will enable us to correlate our present results with the inviscid investigations of Rayleigh and Tollmien, as discussed in Part II.

In all the cases considered, we have $w'' < 0$ for $y < y_2$ but sufficiently near to it. If $w''(y)$ never vanishes for $y_1 < y < y_2$, we can replace w_0'' by w_1'' in the expressions (12.13) and (12.16). In general,

$$w_0'' = w_1'' + \frac{w_1'''}{w_1} c + \left(\frac{w^{iv}}{2w_1^2} - \frac{w_1'' w_1'''}{2w_1^3}\right) c^2 + \cdots .$$

Now, for a flow which is essentially parallel, the boundary condition $\Delta\Delta\psi = 0$, which holds on the solid wall for all two-dimensional laminar flows, can be easily verified to be equivalent to $w_1'' = 0$. Hence, we have

$$w_0' = w_1' + \frac{w^{iv}}{2w_1'^2} c^2 + \cdots .$$

Thus, if $w_1'' = 0$, but w'' does not vanish for $y_1 < y < y_2$, we have

$$R = \{2w_1'^{19}/\pi^2 H_{10}^9 (w^{iv})^2\}\alpha^{-19}, \quad \text{for case (2a)}, \tag{12.18}$$

and

$$R = \{2w_1'^{19}/\pi^2 (w^{iv})^2\}\alpha^{-10}, \qquad \text{for case (3)}. \tag{12.19}$$

In case the velocity profile shows a point of inflection,

$$w_0' = 0 \quad \text{for} \quad c = c_s.$$

Then, we have approximately

$$w_0'' = (w_1^{iv}/2w_1'^2)(c^2 - c_s^2). \tag{12.20}$$

It can now be seen from (12.13) and (12.16) that R becomes infinite as c approaches c_s. Let the corresponding value of α be denoted by α_s. Then instead of (12.18) and (12.19), the following relations hold:

$$R = \{2w_1'^{19}/\pi^2 H_{10}^9 (w_1^{iv})^2\}\alpha^{-11}(\alpha^4 - \alpha_s^4)^{-2}, \quad \alpha_s^2 = w_1' c_s/H_{10}, \text{ for case (2a)}, \tag{12.21}$$

$$R = \{2w_1'^{19}/\pi^2 (w_1^{iv})^2\}\alpha^{-6}(\alpha^2 - \alpha_s^2)^{-2}, \qquad \alpha_s = w_1' c_s, \qquad \text{for case (3)}. \tag{12.22}$$

Thus, for either a symmetrical or a boundary-layer distribution with a flex, we have

$$R \sim (\alpha - \alpha_s)^{-2} \tag{12.23}$$

as $R \to \infty$, $\alpha \to \alpha_s$, $c \to c_s$. In all these approximations, we *assume α_s and c_s to be so small* that the previous approximations still hold, but the qualitative nature of our conclusions cannot be changed for moderate values of α_s and c_s.

The general characteristics obtained from our foregoing discussions are summarized in Table II, and are indicated by the asymptotic branches of the solid lines in Fig. 9. Let us proceed to discuss their significance.

i) It may be expected that the region between the two asymptotic branches of the curves represents a region of instability. Thus, *every symmetrical or boundary-layer profile is unstable for sufficiently large values of the Reynolds number.* This point will be substantiated below.

ii) In the cases where $w_1'' > 0$, the two branches of curves approach the two different asymptotes $\alpha = 0$ and $\alpha = \alpha_s$, leaving a *finite instable region* for infinite Reynolds number. In the other cases, the two branches approach the same asymptote $\alpha = 0$, leaving only the possibility of a neutral disturbance of infinite wave-length at infinite Reynolds number. These results agree with Heisenberg's criterion and the results obtained from the considerations of an inviscid fluid in Part II of this work. It thus appears that the inviscid disturbance with $\alpha = 0$, $c = 0$ is actually not as trivial as it may first appear to be, for it is actually the limiting case of neutral disturbances in a real fluid.

c) *Existence of self-excited disturbances.** To establish the actual existence of self-excited disturbances, we try to show that $c_i > 0$ at least in the neighborhood of the neutral curve. Indeed, we may regard c as a function of the two independent parameters α and $R' = \alpha R$, and show that $(\partial c_i/\partial R')_\alpha < 0$ for the first branch of the curve. This is analogous to Heisenberg's criterion, and demonstrates the same general conclusion that the effect of viscosity is destabilizing at large Reynolds numbers. To fix our ideas, we shall carry out the analysis for the case of symmetrical profiles. The other case can be carried out in a similar manner.

We begin with the equation

$$\frac{f_2(\alpha, c)}{f_4(\alpha, c)} = \frac{\phi_{31}}{\phi_{31}'} \tag{6.14}$$

where $f_2(\alpha, c)$ and $f_4(\alpha, c)$ are given by (6.26) and ϕ_{31}/ϕ_{31}' is given by (6.28). By using those relations, we can transform (6.14) into

* This section was inserted late in 1944 after discussions with Prof. C. L. Pekeris. He mentioned the possibility that the neutral curve might be a curve of minimum damping with stable regions on both sides of it. See also Schlichting's calculations [52].

$$\mathcal{F}(z) = \phi_{22}' \Big/ \left(\phi_{22}' + \frac{1}{w_1' c}\phi_{12}'\right);$$

or, by further using (6.30) and (6.24),

$$\mathcal{F}(z) - 1 = w_1' c \sum_{n=1}^{\infty} \alpha^{2n} K_{2n}(c) \Big/ \sum_{n=1}^{\infty} \alpha^{2n} H_{2n-1}(c).$$

We now regard α as fixed and consider the variation of c with R' or z, which is a known function of c and R'. Taking logarithmic derivatives on both sides, we have

$$\frac{\mathcal{F}'(z)}{\mathcal{F}(z) - 1} = \left\{\frac{1}{c} + \frac{\sum_{n=1}^{\infty} \alpha^{2n} K_{2n}'(c)}{\sum_{n=1}^{\infty} \alpha^{2n} K_{2n}(c)} - \frac{\sum_{n=1}^{\infty} \alpha^{2n} H_{2n-1}'(c)}{\sum_{n=1}^{\infty} \alpha^{2n} H_{2n-1}(c)}\right\} \frac{dc}{dz}. \tag{12.24}$$

So far, α, c, and z are arbitrary. On the neutral curve, c and z are real, and we may use the relation (12.13) if we are on the first branch of the neutral curve with large values of R'. Indeed, for large values of z, (12.6) gives

$$\frac{\mathcal{F}'(z)}{\mathcal{F}(z) - 1} = -\frac{3}{2z}$$

and

$$-\frac{3dz}{2z} = -\frac{1}{2}\frac{dR'}{R'} - \frac{3}{2}\frac{dc}{c}.$$

By using these relations, it can be easily verified that (12.24) leads to

$$\frac{dR'}{2R'} - \frac{3dc}{2c} = dc\left\{\frac{1}{c} + \frac{\sum_{n=1}^{\infty} \alpha^{2n} K_{2n}'(c)}{\sum_{n=1}^{\infty} \alpha^{2n} K_{2n}(c)} - \frac{\sum_{n=1}^{\infty} \alpha^{2n} H_{2n-1}'(c)}{\sum_{n=1}^{\infty} \alpha^{2n} H_{2n-1}(c)}\right\}.$$

Remembering that $c = O(\alpha^2)$ and noting that

$$K_1(c) = -\frac{1}{w_1 c} - \frac{w_0''}{w_0'^3}(\log c + i\pi) + O(1),$$

where $O(1)$ is real, we can reduce the above equation to

$$\frac{dR'}{2R'} + \frac{3dc}{2c} = dc\left\{1 + w_1' c \frac{w_0''}{w_0'^3}(\log c + i\pi)\right\}^{-1} \frac{d}{dc}\left\{\frac{w_1' c w_0''}{w_0'^3}(\log c + i\pi)\right\},$$

or

$$\frac{1}{2}\frac{dR'}{R'} = -\frac{3dc}{2c}\left\{1 + c\frac{d}{dc}\left[\frac{w_1' c w_0''}{w_0'^3}(\log c + i\pi)\right]\right\}. \tag{12.25}$$

For small values of c, the expression in the brackets has a positive real part and a negative imaginary part. Hence, $(\partial c/\partial R')_\alpha$ has a negative imaginary part. This completes the proof. Indeed, if w_1'' does not vanish, we have

$$\left.\begin{aligned}\left(\frac{\partial c_r}{\partial R'}\right)_\alpha &= -\frac{c}{3R'} \sim R'^{-6/5},\\ \left(\frac{\partial c_i}{\partial R'}\right)_\alpha &= \frac{2\pi w_1''}{9w_1'}\frac{c^2}{R'} \sim R'^{-7/5}.\end{aligned}\right\} \tag{12.26}$$

In the above derivation, it should be noted that all approximations are made by neglecting small terms of higher orders in *comparison* with some terms which have been retained. Thus, the conclusion of stability or instability would not be altered by those terms of higher orders.

d) *The minimum critical Reynolds number and the minimum critical wave-length.* Having demonstrated the instability of the symmetrical and the boundary-layer profiles, we want to answer the following questions. First, does there exist a minimum critical Reynolds number, below which the flow is stable for disturbances of all wave-lengths? If so, can we get an approximate estimate of its magnitude? Secondly, does there exist a minimum wave-length of the disturbance (maximum α) below which the flow is stable at all Reynolds numbers? If so, can we get an approximate estimate of its magnitude? We shall see that in trying to answer these questions, we can also roughly depict the complete $\alpha(R)$ curve, which separates stability from instability.

The existence of these minimum values can be most conveniently inferred from a condition of stability derived by Synge* from energy considerations. His condition reads

$$(qR)^2 < (2\alpha^2 + 1)(4\alpha^4 + 1)/\alpha^2, \qquad q = \max \left| w' \right|. \tag{12.27}$$

This condition insures the existence of a minimum critical Reynolds number. It permits α to become infinite only for $R \to \infty$. But we know from our previous considerations that $\alpha \to \alpha_s$ or 0 as $R \to \infty$. Hence, we would expect that there exists a maximum value of α, above which there is always stability. The neutral curve must therefore take the general shape shown in Fig. 9. The asymptotic behaviors of the solid curves are drawn in qualitative accordance with (12.6), (12.7), and (12.23); the other parts of the solid curves are arbitrarily drawn to indicate the general shape of the curve. It is evident that the region outside the curve is the region of stability, and the enclosed region is the region of instability. Similar conclusions have been reached by Heisenberg† but his arguments and results appear to be somewhat obscure.

Having established the existence of the minimum critical value of R and the maximum critical value of α, we proceed to make an estimate of their magnitude. We shall see that our theory permits us to give a quite good approximation to the minimum value of αR (cf. (12.30)). Since this roughly corresponds to the minimum value of R and also to the maximum value of α (as will be clear from the individual examples given below), we can get a rough estimate of these values by making a rough estimate of α corresponding to the minimum value of αR.

Using the second equation of (8) of Appendix and the approximation (12.7) for v, we have approximately

$$\mathcal{F}_i(z) = v(c) = -\pi w_1' \frac{ww''}{w'^3}. \tag{12.28}$$

* Synge, [63], eq. (11.23), p. 258. His λ is our α. The condition is originally stated for plane Couette and plane Poiseuille motion; but it is easily seen that it holds for a general velocity distribution with $q = \max|w'|$.

† Heisenberg, loc. cit., p. 601.

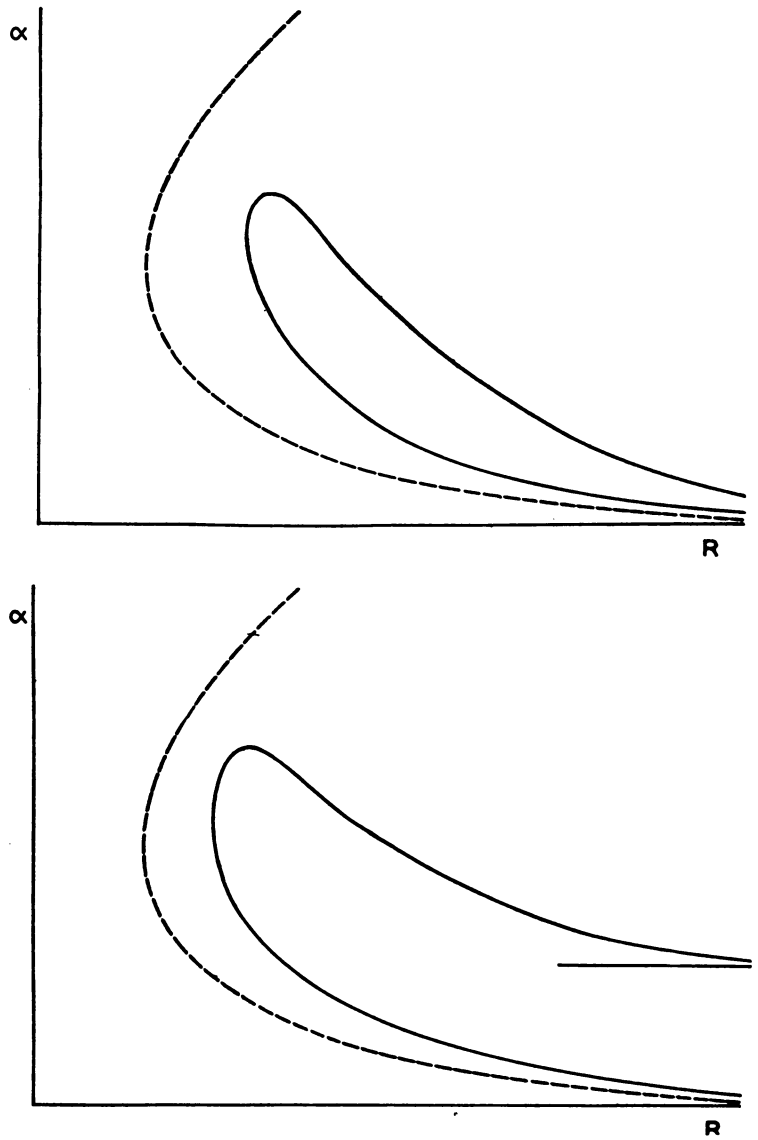

FIG. 9. General nature of the curve of neutral stability. The dotted curve is curve of stability given by Synge.

If we recall that z is proportional to $c(\alpha R)^{1/3}$, this equation determines $(\alpha R)^{1/3}$ as a function of c. It can then be easily verified that the minimum value of $(\alpha R)^{1/3}$ occurs when

$$z\mathcal{F}_i'(z) = cv'(c). \tag{12.29}$$

If the point where this holds is denoted by $z = z_0$, we have approximately from (11.28)*

$$\alpha R = w_1'^2\left(\frac{z_0}{c}\right)^3. \tag{12.30}$$

* Cf. Heisenberg, loc. cit., eq. (29a), p. 602. He put $z_0 \sim 1$.

The point z_0 is roughly the value where $\mathcal{J}_i(z)$ takes its maximum value, because (12.29) is approximately $\mathcal{J}_i'(z)=0$, when c is small. The corresponding value of α can be approximately obtained by taking

$$u = \mathcal{J}_r(z_0), \tag{12.31}$$

in accordance with the first equation of (8) of Appendix, where u is given by the real part of (5) or (7) of Appendix, as the case may be.

e) *Approximate rules.* We now proceed to make some rough approximations in order to obtain simple rules, which are convenient for estimating the minimum critical Reynolds number. The condition $\mathcal{J}_i'(z_0)=0$ gives $z_0=3.21$, where $\mathcal{J}_r(z_0)=1.49$ and $\mathcal{J}_i(z_0)=0.58$. The corresponding value of c can be obtained from the second equation of (8) of Appendix. Putting $u=1.5$ in accordance with (12.31) and neglecting second order terms of λ, we have

$$v(1-2\lambda) = \mathcal{J}_i(z_0) = 0.58,$$

i.e.,

$$-\pi w_1'(1-2\lambda)(ww''/w'^3) = 0.58, \tag{12.32}$$

where λ is defined by (4) of the Appendix. To find the value of c from this equation, it is convenient to plot its left-hand side together with $w(y)$ against y, and read the value off the latter curve where the former curve gives the value 0.58. The value of c so obtained turns out to be very close to its maximum value along the neutral curve, and is approximately the value where R is a minimum.

The values of α and R must be obtained from more rough approximations. With a consultation of the values of the integrals $H(c)$, $K(c)$, $M(c)$ and $N(c)$ given in the Appendix, we may derive the following reasonable estimates of α:

$$\alpha^2 = w_1' c/H_{10}, \qquad H_{10} = \int_{y_1}^{y_2} w^2 dy, \quad \text{for symmetrical profiles,} \tag{12.33}$$

$$\alpha = w_1' c, \qquad \text{for boundary layer profiles.} \tag{12.34}$$

These values turn out to be somewhat lower than the accurate values. With an approximate allowance for these inaccuracies and taking round numbers, we get the following approximate rules for the minimum critical Reynolds number:

$$R = \frac{30 w_1'}{c^3}\sqrt{\frac{H_{10}w_1}{c}}, \quad \text{for symmetrical profiles,} \tag{12.35}$$

$$R = \frac{25 w_1'}{c^4}, \qquad \text{for boundary layer profiles.} \tag{12.36}$$

The calculations have been carried out for the Blasius case and the plane Poiseuille case. In the first case, the thickness of the boundary layer is taken so that the initial slope is $w_1'=2$. It is found that

$$\left.\begin{aligned} R &= 5906 \quad \text{for Poiseuille case,} \\ R\delta_1 &= 502 \quad \text{for Blasius case.} \end{aligned}\right\} \tag{12.37}$$

The quantity δ_1 is the displacement thickness

$$\delta_1 = \int_0^\infty (1-w)dy = 0.28673,$$

where y is measured from the solid wall. These values for the minimum critical Reynolds number agree fairly well with those obtained below from more elaborate numerical calculations.

When these estimates of the minimum values of R and the corresponding values of α (eqs. (12.32)–(12.36)) are combined with the asymptotic behavior of the $\alpha(R)$ curves (eqs. (12.16)–(12.17)), the curve of neutral stability in any case can be sketched with fair accuracy with very little labor.

The maximum value of α on the neutral curve cannot be very well estimated. It is usually somewhat higher than the values of α given by (12.33) and (12.34).

13. Stability characteristics of special velocity distributions. We shall now apply our theory to some special cases in order to obtain numerical results comparable with experiments. We take (a) the Blasius case as a typical boundary-layer profile, and (b) the plane Poiseuille motion as a typical symmetrical profile. In any case, the resultant curve of stability limit should have the general shape discussed in the last two sections. Only the results will be given here; the method of calculation and its accuracy will be discussed in the Appendix.

a) *Stability of plane Poiseuille flow.* The velocity distribution of plane Poiseuille motion is given by

$$w(y) = 2y - y^2, \quad \text{with} \quad w_1' = 2, \quad H_1(0) = 8/15. \tag{13.1}$$

TABLE II. Behavior of $R(\alpha)$ Curve for Large Values of R for Velocity Distributions with $w''<0$ for the Main Part of the Profile.

	First branch			Second branch
	$w_1''<0$	$w_1''=0$	$w_1''>0$	
Symmetrical profile	α^{-11}	α^{-19}	$(\alpha-\alpha_s)^{-2}$	α^{-7}
Boundary-layer profile	α^{-6}	α^{-10}	$(\alpha-\alpha_s)^{-2}$	α^{-4}

The two branches of the $\alpha(R)$ curve are given by (cf. (12.13), (12.14))

$$\left.\begin{aligned} R^{1/3} &= 8.44(\alpha^2)^{-11/6}, \quad c = 4\alpha^2/15; \\ R^{1/3} &= 5.96(\alpha^2)^{-7/6}, \quad c = 0.611\alpha^2. \end{aligned}\right\} \tag{13.2}$$

The numerical results are shown in Table III and Fig. 10. The significance of the column s in the table will be explained in the next section. From the figure, we see that the minimum critical Reynolds number occurs at $R^{1/3}=17.45$, or $R=5314$, agreeing very well with our previous estimation.*

Earlier results. The stability of plane Poiseuille flow has been attempted by many authors. Comparatively recent papers are those of Heisenberg, [14], Noether [36], Goldstein [6], Pekeris [39, 40], Synge [64], and Langer [25]. The papers of Goldstein and Synge and one of the papers of Pekeris [39] give definite indication of stability at sufficiently low Reynolds numbers. Heisenberg's paper is in general agreement

* The values given here are somewhat different from those published before [27], because the computation of Tietjen's function has been revised.

with the present investigations. He gave only a very rough calculation, whose result is reproduced in the figure. It seems that his curve is

$$R^{1/3} = 13.4(\alpha^2)^{-11/6}.$$

This is different from our present result (13.2) by a numerical factor. It may be noted

TABLE III. Stability of Plane Poiseuille Flow.

c	z	α	R	s	α^2	$R^{1/3}$
0	2.294	0	∞	.7214	0	∞
0.05	2.363	0.3056	13.64×10^5	.6901	0.0934	110.91
0.10	2.448	0.4603	1.243×10^5	.6544	0.2119	49.90
0.15	2.540	0.6024	31048	.6192	0.3629	31.43
0.20	2.668	0.7506	12024	.5752	0.5634	22.91
0.25	2.868	0.9263	6108	.5161	0.8580	18.28
0.266	3.012	1.0101	5369	.4795	1.0203	17.51
0.270	3.080	1.0414	5314	.4637	1.0845	17.45
0.272	3.21	1.0836	5659	.4358	1.1741	17.82
0.270	3.240	1.0888	5920	.4298	1.1854	18.09
0.266	3.320	1.1007	6602	.4144	1.2115	18.76
0.25	3.495	1.1033	9287	.3836	1.2173	21.02
0.20	3.857	1.0254	26597	.3309	1.0514	29.85
0.15	4.152	0.8824	92529	.2963	0.7787	45.23
0.10	4.458	0.6990	4.9435×10^5	.2663	0.4886	79.07

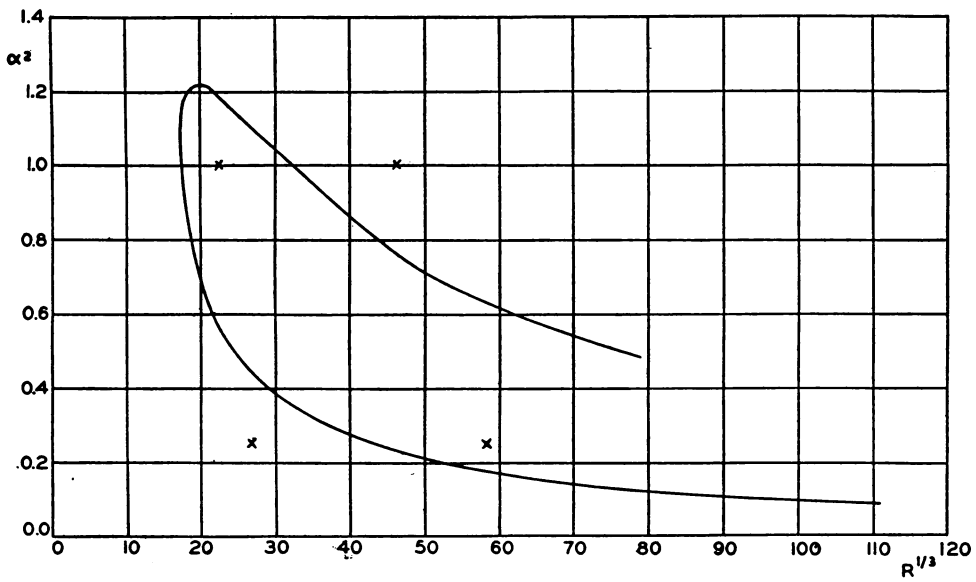

FIG. 10. Curve of neutral stability for the plane Poiseuille case.

that for the values of α for which his curve is drawn, the approximation used in deriving (13.2) is no longer legitimate. Noether's work is based upon a very good mathematical approach, which seems to promise further developments. However, in apply-

ing his method to particular examples, he neglected the terms in α^2 in the inviscid solutions. As is evident from previous discussions, this is bound to lead to the wrong conclusion that the plane Poiseuille flow is stable (as Noether actually did). The mathematical analysis in Langer's work shows that the region of the c-plane for which $c_i > 0$ must go to zero as αR becomes infinite. This is in agreement with present results. Langer, however, concluded from his analysis that the motion is probably stable in general. This would be a natural deduction if the effect of viscosity were only *stabilizing*. The instability of the plane Poiseuille flow must therefore be attributed to the destabilizing effect of viscosity. This is a very significant fact and will be discussed in greater detail in §14.

Pekeris' second paper [40] is a numerical treatment of (4.1), replacing a derivative by a ratio of two finite differences. Unfortunately, his method is not suitable for the purpose, because he has virtually *neglected the inner friction layer*. In his approximation, he divided the half-width of the channel into (at most) four equal parts corresponding to $w = 0$, 7/16, 3/4, 15/16, 1. From the present work, we know that the inner friction layer occurs definitely for $c < 6/16$. We know also from our previous investigations that the function ϕ varies very rapidly in the neighborhood of the inner friction layer. Hence, it is not legitimate to replace ϕ' by $\Delta\phi/\Delta y$ for the interval (0, 1/4), y being measured from the solid wall here. Also, most of the combinations of values (α, R) he selected do not correspond to a strong instability. These values are marked with crosses in Fig. 10.

b) *Stability of Blasius flow.* For this case, we choose the boundary-layer thickness to be defined by

$$\tilde{y} = \tilde{\delta} = 6\tilde{x}/\sqrt{R_x}, \qquad R_x = \tilde{u}_1\tilde{x}/\nu, \tag{13.3}$$

where $\tilde{x}$, $\tilde{y}$ are the *dimensional* distances from the leading edge and the wall respectively, and $\tilde{u}_1$, ν are the *dimensional* free stream velocity and the kinematic viscosity respectively.* With this definition, the dimensional displacement thickness is

$$\tilde{\delta}_1 = 0.28673\tilde{\delta}. \tag{13.4}$$

Such a choice has the convenience that the initial part of the velocity curve can be very accurately represented by

$$w(y) = 2y - 3y^4, \tag{13.5}$$

y being measured from the wall. Also, since the edge of the boundary layer is farther from the solid wall than that set by Tollmien and Schlichting, greater accuracy can be expected. To make it easy to compare with other results, all final values are presented in terms of

$$\alpha_1 = \alpha\delta_1, \qquad R_1 = R\delta_1. \tag{13.6}$$

The two asymptotic branches of the $\alpha(R)$ curve are given by the following formulae (cf. (12.16) and (12.17)):

$$R_1 = 2.21(10)^{-5}\alpha_1^{-10}, \qquad c = 1.74\alpha_1, \tag{13.7}$$

$$R_1 = 0.0622\alpha_1^{-4}, \qquad c = 4.00\alpha_1. \tag{13.8}$$

* Cf. Goldstein [7], vol. I, p. 135.

These formulae may be compared with those given by Tollmien.* The complete numerical result is shown in Table IV and Fig. 11. The minimum critical Reynolds number occurs at $R_1=420$, agreeing fairly well with our previous estimation and the earlier results of Tollmien and Schlichting.

TABLE IV. Stability of Blasius Flow.

c	z	α	R	s	α_1	R_1
0	2.294	0	∞	.7214	0	∞
0.05	2.294	0.0473	81.45×10^5	.7214	0.0136	23.353×10^5
0.10	2.296	0.1040	4.655×10^5	.7205	0.0298	1.335×10^5
0.15	2.311	0.1730	84555	.7135	0.0496	24244
0.20	2.341	0.2588	24783	.6998	0.0742	7106
0.25	2.396	0.3693	9536	.6759	0.1059	2734
0.30	2.481	0.5156	4388	.6414	0.1478	1258
0.35	2.624	0.7149	2358	.5897	0.2050	676
0.40	2.942	1.0778	1477	.4967	0.3090	423
0.411	3.21	1.2968	1470	.3459	0.3718	421
0.40	3.540	1.4264	1944	.3763	0.4090	557
0.35	4.219	1.2992	5392	.2893	0.3725	1546
0.30	4.382	1.0055	12399	.2733	0.2883	3555
0.25	4.685	0.7578	34739	.2472	0.2173	9961

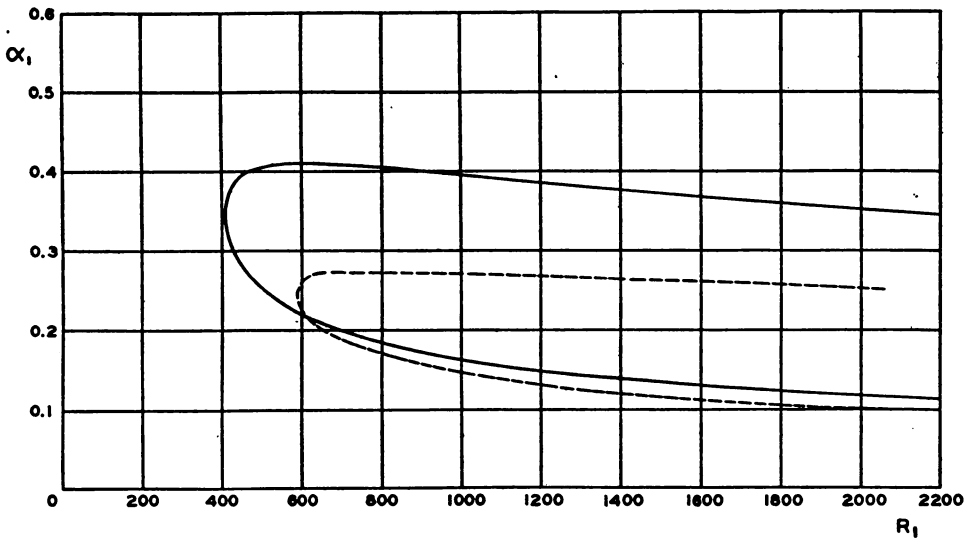

FIG. 11. Curve of neutral stability for the Blasius case:
——— present calculation, – – – Schlichting's calculation.

Earlier results. The stability of the boundary layer has been calculated by Tollmien and later by Schlichting, approximating the velocity distribution by linear and parabolic distributions. For the evaluation of the imaginary part corresponding to the inviscid solutions, they used the exact profile. The calculation of Schlichting is shown dotted in the figure. Tollmien's curve agrees fairly well with the present calculations,

* Loc. cit. [73], first paper, p. 42.

except for a somewhat lower peak. Schlichting also calculated the amplification of the unstable disturbances [52], and the amplitude distribution and energy balance of the neutral disturbances [54]. Since the neutral curve in his calculation is inexact, it might be desirable to repeat some of his work if experimental results were available. For those calculations, the present scheme promises less numerical labor than Schlichting's original work.

14. Physical significance of the results. Prospect of further developments. Let us now summarize all the results which have been obtained and discuss their physical significance. In the first place, we may conclude that all the inertia forces controlling the stability of two-dimensional parallel flows can be considered in terms of the distribution of vorticity. If the gradient of vorticity of the main flow does not vanish inside the fluid, then self-excited disturbances cannot exist except through the effect of viscosity.

In fact, the effect of viscosity is in general *destabilizing* for very large Reynolds numbers. Thus, if a wavy disturbance of *finite* wave-length can exist neutrally for an inviscid fluid, it will be *amplified through the effect of viscosity*. Indeed,* if the Reynolds number of a flow is continually decreased, a disturbance of finite wave-length, which is damped at very large Reynolds numbers, becomes amplified, unless the wave-length is so small as to cause excessive dissipation at any Reynolds number. For still smaller Reynolds numbers, the damping effect becomes predominant, and we have again a decay of the disturbance. However, for the particular disturbance of infinite wave-length (essentially a steady deviation), the effect of viscosity may be said to be always of the nature of a damping.

The effect of viscosity is essentially one of diffusion of vorticity. It can be seen more clearly from the following considerations. Let us imagine a disturbance originating from the inner friction layer where the phase velocity of the disturance is equal to the velocity of the main flow. During one period $2\pi l/\alpha c U$ of the disturbance, the viscous forces will propagate it side-wise through a distance of the order $\sqrt{2\pi\nu l/\alpha c U} = l\sqrt{2\pi/\alpha R c}$. It is significant to compare this distance with the distance between the inner friction layer and the solid boundary. For if they are nearly equal, it means that the effect of viscosity is dominant at least from the solid surface to that layer. This ratio is approximately

$$s = \sqrt{2\pi/z^3} \tag{14.1}$$

where z is defined by (6.28). This quantity may be regarded as a measure of the effect of viscosity. Its value is included in Tables III and IV. We notice that the value of s decreases from 0.7 to 0.5 as we follow the lower branch of the neutral curve of stability from infinite Reynolds number to the minimum critical Reynolds number. Then, as s decreases to zero, we are following the other branch of the neutral curve to infinite Reynolds numbers. Thus (see Figs. 9, 10, 11), the lower branch is essentially controlled by the effect of viscosity. The effect here is stabilizing, since an increase of Reynolds number gives instability. On the other branch, the effect of viscosity on diffusion of vorticity is predominant in comparison with the effect of dissipation. Here, an increase of Reynolds number gives stability; i.e., the effect of viscosity is destabilizing. This destabilizing mechanism is essentially to shift the phase difference between the u and v components of the disturbance. It has been ex-

* See Fig. 9.

plained in some detail in Prandtl's article [42] from the point of view of energy balance.

If we consider disturbances from the wall and from the inner friction layer, we may regard the region in between to be wholly governed by the effect of viscosity, if these disturbances meet after a period. Thus, it is not without significance that the minimum critical Reynolds number occurs for $s=\frac{1}{2}$ approximately, which may be regarded as marking the passage from stabilizing effect to destabilizing effect of the viscous forces.

These discussions hold both for symmetrical velocity distributions and for boundary-layer distributions. In both cases, it has been demonstrated that instability is essentially caused by the effect of viscosity. These velocity distributions are unstable whether a point of inflection occurs in the velocity profile or not. Thus, although the gradient of vorticity plays a part in controlling the stability of the flow, it is by no means the dominant factor, particularly at low Reynolds numbers. There is thus no reason to associate a point of inflection in the profile directly with instability. This removes Taylor's objection of instability theories based on von Doenhoff's experiments.* Even if the point of inflection in the velocity profile occurs in the leading part of the plate in his experiments, the flow there is definitely stable.

There is another objection raised by Taylor against Tollmien's work on the stability of the boundary layer. He questions whether the change of boundary-layer thickness should not have a drastic influence. This point can best be settled experimentally. So far as mathematical considerations are concerned, it seems justifiable to consider a boundary layer as a parallel flow; the fractional variation of thickness is very small over a distance of one wave-length of the disturbance, and the error incurred is only a few per cent. A fuller discussion of all the errors involved in the theory will be given in the Appendix.

Another point should be settled by experimental investigations. Since the general impression had been that the plane Poiseuille flow was stable, Prandtl suggested that instability occurred at the entrance flow where the velocity distribution is not yet parabolic. The present work certainly concludes that such entrance flows are unstable, if they can be considered as approximately parallel. It is hard to decide theoretically whether a well-developed turbulence has already been reached before the parabolic profile is established. This presumably depends upon the conditions of disturbance at the inlet. The question can be best settled experimentally.

Of the six types of problems mentioned in section 3, Part I, the three types (1), (2), and (5) seem to be quite settled. The present work on the boundary layer checks Tollmien's result approximately, with a minimum critical Reynolds number $R_1=R\delta_1=420$. The minimum critical Reynolds number for plane Poiseuille flow is found to be 10600 based upon the width of the channel. These values are at least not in disagreement with the existing experimental results. It would be very interesting if experiments could be carried out to check the theoretical results so far obtained.

Since plane Couette motion is concluded to be stable while plane Poiseuille motion is concluded to be unstable, it seems interesting to investigate a combination of them to find out when does the instability begin as one changes both the pressure gradient and the relative motion of the plates.

* Taylor, loc. cit. [70], p. 308.

The stability of two-dimensional jets and wakes has never been investigated with the effect of viscosity included. It seems that a study of the stability of the two-dimensional wake might give us valuable information regarding the von Kármán vortex street,—particularly regarding the minimum Reynolds number of its occurrence and the width of the street as compared with the size of the body.*

Transition to turbulence. The success of Taylor's theory of transition [68, 70] to turbulence in the boundary-layer as caused by external turbulence seems to throw the instability theories at a disadvantage. However, it seems that Taylor's work should be regarded as only one phase of the problem, i.e., concerning cases where the external turbulence plays the dominant role. In fact, it is not impossible to construct an instability theory, taking account of the free turbulence outside the boundary-layer if this is the main cause of transition. The boundary condition $\phi'+\alpha\phi=0$ at the edge of the boundary layer signifies that the disturbance there has equal magnitudes in directions parallel and perpendicular to the wall. This can be easily reconciled with the nearly isotropic turbulence in the free stream. Of course, the theory can only be pushed to the point where *non-linear* effects *begin* to appear. Otherwise, we have to deal with a very difficult mathematical problem. It is possible that the beginning of non-linear effect is not far from the actual point of transition. Then the instability theory should give useful results regarding transition, which might be expected to check with experiment.

Appendix

In the following paragraphs, we shall describe the methods by which the numerical calculations are carried out. We shall then give a discussion of the numerical accuracy involved in the calculations. Special emphasis will be placed on the case of Blasius flow.

a) *Transformation of equations.* The basic equations for the determination of the stability characteristics are given at the end of Part I. To carry out the numerical calculation in any particular case, we have to evaluate the functions (6.24) which occur in the equations (6.14), (6.15) and (6.17) through the relations (6.26). It is found convenient to transform (6.24) into

$$\left.\begin{aligned}
\phi_{12} &= (1-c)(1-\alpha^2H_2)^{-1}\left(1-\sum_{n=2}^{\infty}\alpha^{2n}M_{2n}\right),\\
\phi_{22} &= K_1\phi_{12}-(1-c)\sum_{n=0}^{\infty}\alpha^{2n}N_{2n+1},\\
\phi'_{12} &= (1-c)(1-\alpha^2H_2)^{-1}\left(\alpha^2H_1-\sum_{n=2}^{\infty}\alpha^{2n}M_{2n-1}\right)+(1-c)^{-1}w_2'\phi_{12},\\
\phi'_{22} &= K_1\phi'_{12}+(1-c)^{-1}\left(1-\sum_{n=1}^{\infty}\alpha^{2n}N_{2n}\right)+(1-c)^{-1}w_2'\phi_{22},
\end{aligned}\right\} \tag{1}$$

where the functions $M_n(c)$ and $N_n(c)$ are defined by

$$\left.\begin{aligned}
M_n &= H_n-H_2H_{n-2}, \qquad n\geqq 3,\\
N_n &= K_n-K_1H_{n-1}, \qquad n\geqq 2.
\end{aligned}\right\} \tag{2}$$

* This problem has been attempted by Heisenberg; see Goldstein's book [7].

The principal advantages of such transformations is to bring out the dominant terms in the functions ϕ_{12}, ϕ_{12}', ϕ_{22} and ϕ_{22}'. For the terms in M's and N's are usually very small (particularly for small values of c, with which we are usually concerned), while all the terms in the series of (6.24) are of considerable importance. This point will be fully discussed below.

The calculation of (6.13) (Case 1) is still quite complicated; it is found necessary to take (6.15) (Case 2b) as a first approximation. Since we are not going to make any actual calculation for this case, we shall not go into further details with (6.13). All the other equations (6.14), (6.15), and (6.17) (Cases 2a, 2b, 3) can be transformed into the form

$$\mathcal{J}(z) = \frac{(1+\lambda)(u+iv)}{1+\lambda(u+iv)}, \tag{3}$$

with $\mathcal{J}(z)$ defined by (6.31) and $\lambda = \lambda(c)$ defined by

$$w_1'(y_1 - y_0) = -c(1+\lambda). \tag{4}$$

Thus, λ is usually very small. The quantities u and v are real functions of α and c, different for different cases. For Case 2a we have

$$\begin{aligned} u+iv &= 1+w_1'c\phi_{22}'/\phi_{12}' \\ &= w_1'c\left(K_1+\frac{1}{w_1'c}\right) \\ &\quad +\frac{w_1'c}{\alpha^2}(1-\alpha^2H_2)(1-\alpha^2H_2-\alpha^4N_4-\cdots)(H_1-\alpha^2M_3-\alpha^4M_5-\cdots)^{-1}, \end{aligned} \tag{5}$$

where the second form of the right-hand side is derived by using (1). Similarly, for Cases 2b and 3, we have, respectively,

$$\begin{aligned} u+iv &= 1+w_1'c\phi_{22}/\phi_{12} \\ &= w_1'c\left(K_1+\frac{1}{w_1'c}\right) \\ &\quad +w_1'c\alpha^2(1-\alpha^2H_2)(1-\alpha^4M_4-\alpha^6M_6-\cdots)^{-1}(N_3+\alpha^2N_5+\cdots) \end{aligned} \tag{6}$$

and

$$\begin{aligned} u+iv &= 1+w_1'c(\phi_{22}'+\alpha\phi_{22})/(\phi_{12}'+\alpha\phi_{12}) \\ &= w_1'c\left(K_1+\frac{1}{w_1'c}\right) \\ &\quad +\frac{w_1'c}{\alpha^2}\,\frac{(1-\alpha^2H_2)\{(1-\alpha^2H_2-\alpha^4N_4-\cdots)-(1-c)^2(\alpha^3N_3+\alpha^5N_5+\cdots)\}}{(1-c)^2(1-\alpha^4M_4-\alpha^6M_6-\cdots)+\alpha(H_1-\alpha^2M_3-\cdots)}. \end{aligned} \tag{7}$$

Equation (3) contains the two real equations

$$\left.\begin{aligned} \mathcal{J}_r(z) &= (1+\lambda)\{u(1+\lambda u)-\lambda v^2\}\{(1+\lambda u)^2+(\lambda v)^2\}^{-1}, \\ \mathcal{J}_i(z) &= (1+\lambda)v\{(1+\lambda u)^2+(\lambda v)^2\}^{-1}, \end{aligned}\right\} \tag{8}$$

for z, α, c. Thus, for each value of z, we can determine corresponding values of α and c. Finally, the Reynolds number is given by (cf. (6.28))

$$\alpha R = \frac{1}{w_0'(1+\lambda)^3}\left(\frac{w_1' z}{c}\right)^3. \tag{9}$$

The actual procedure of calculation will be described presently.

b) *Procedure of calculation.* The calculations required in §13 are as follows: (a) to find the values of α and z corresponding to each value of c by using equations (8), with u and v defined by (7) and (9); and (b) to calculate R from (9). To do this, we may take the following procedure. We first plot $\mathcal{J}_i$ against $\mathcal{J}_r$; then plot the corresponding right-hand side members of (8) in a similar manner in the same diagram. Noting that the latter are functions of α and c only, we may plot by drawing curves of constant α (or constant c). The intersections of this set of curves with the $(\mathcal{J}_r, \mathcal{J}_i)$ curve give the desired results.

This procedure is however, very laborious. A simpler method is as follows: As will be seen below, the imaginary parts of H's, M's and N's appearing in (5) and (7) are very small compared with that of $K_1(c)$, we can therefore use the approximation

$$v = v(c) = -\pi w_1'(ww''/w'^3) \quad \text{for} \quad w = c. \tag{10}$$

The following steps are then taken:

i) *Calculation of* αR. In this step, the auxiliary functions

$$\lambda(c),\ w_0'(c),\ v(c)$$

are required. These are tabulated in Tables V and VI for the cases considered. Having calculated these functions, we can determine z and u for each value of c; αR is then

TABLE V. Auxiliary Functions for Calculating the Stability of the Plane Poiseuille Flow.

c	w_0'	λ	v	$w_1' cRl$	H_1	H_2	M_3	N_3
0	2	0	0	0	0.53333	0.21817	0.06038	0.19340
0.05	1.94936	0.01282	0.08482	0.06499	0.46917	0.20696	0.05047	0.20401
0.10	1.89737	0.02633	0.18397	0.10187	0.41000	0.19516	0.04183	0.21636
0.15	1.84391	0.04061	0.30066	0.13015	0.35583	0.18276	0.03441	0.22777
0.20	1.78885	0.05573	0.43905	0.15351	0.30667	0.16982	0.02813	0.23918
0.25	1.73205	0.07180	0.60460	0.17356	0.26250	0.15626	0.02293	0.25000
0.30	1.67332	0.08893	0.80463	0.19121	0.22333	0.14209	0.01872	0.26191
0.35	1.61245	0.10728	1.04910	0.20699	0.18917	0.12729	0.01540	0.27000
0.40	1.54919	0.12701	1.35193	0.22130	0.16000	0.11182	0.01282	0.27062
0.45	1.48324	0.14836	1.73296	0.23438	0.13583	0.09563	0.01087	0.26232
0.50	1.41421	0.17157	2.22144	0.24645	0.11667	0.07875	0.00937	0.23366

determined from (9). In actual practice, a procedure of successive approximations is used. By taking

$$u^{(0)} = \mathcal{J}_r(z^{(0)}), \qquad z = z^{(0)}, \qquad \mathcal{J}_r^{(0)} = \mathcal{J}_r(z_r^{(0)}), \qquad \mathcal{J}_i^{(0)} = \mathcal{J}_i(z^{(0)}) = v$$

as the initial approximation for u, z, $\mathcal{J}_r$, $\mathcal{J}_i$, we can obtain the successive approximations by the formulae

$$\begin{cases} \mathcal{J}_i^{(n+1)} = v\{1+\lambda\}\{(1+\lambda u^{(n)})^2 + (\lambda v)^2\}^{-1} \\ u^{(n+1)} = \mathcal{J}_r^{(n+1)}\{(1+\lambda u^{(n)})^2 + (\lambda v)^2\}\{(1+\lambda)(1+\lambda u^{(n)})\}^{-1} + \lambda v(1+\lambda u^{(n)})^{-1}. \end{cases}$$

TABLE VI. Auxiliary Functions for Calculating the Stability of Blasius Flow.

c	v	$w_1' cRl$	H_1	H_2	M_3	N_3
0	0	0	0.60260	0.23513	0.07966	0.17615
0.05	0.00088	0.02194	0.53378	0.22392	0.06975	0.18676
0.10	0.00709	0.06121	0.46995	0.21212	0.06111	0.19911
0.15	0.02406	0.12108	0.41112	0.19972	0.05369	0.21052
0.20	0.05773	0.20469	0.35730	0.18678	0.04741	0.22193
0.25	0.11498	0.31568	0.30848	0.17322	0.04221	0.23275
0.30	0.20438	0.45835	0.26465	0.15905	0.03800	0.24466
0.35	0.33718	0.63751	0.22583	0.14425	0.03468	0.25275
0.40	0.52839	0.85766	0.19200	0.12878	0.03210	0.25337
0.45	0.79820	1.12133	0.16318	0.11259	0.03015	0.24507
0.50	1.17350	1.42576	0.13935	0.09571	0.02865	0.21641

In each approximation, $\mathcal{J}_r^{(k)}$ and $z^{(k)}$ are determined graphically from $\mathcal{J}_i^{(k)}$.

ii) *Calculation of* α. For this purpose, the additional auxiliary functions

$$w_1' cRl = w_1' cRl\left\{K_1(c) + \frac{1}{w_1' c}\right\},\ H_1(c),\ H_2(c),\ M_3(c),\ N_3(c),\ \cdots$$

are required. These are tabulated in Tables V and VI for the cases considered. The methods of evaluating these functions and their accuracy will be discussed below. For sufficient accuracy in the final results, only the real parts of H_2, M_3, N_3 are required, besides $w_1' cRl$ and H_1. Having calculated these functions, we can determine the value of α from the real part of the equations (5) or (7). A similar method of successive approximations may be used by writing those equations in the forms

$$\alpha^2 = \frac{w_1' c}{H_1(u - w_1' cRl)}(1-\alpha^2 H_2)\,\frac{1-\alpha^2 H_2 - \alpha^4 N_4 - \cdots}{1-\alpha^2 P_2 - \alpha^4 P_4 - \cdots}, \qquad P_{2n} = M_{2n+1}/H_1,$$

$$\alpha = \frac{w_1' c}{u - w_1' cRl}(1-\alpha^2 H_2)\,\frac{(1-\alpha^2 H_2 - \alpha^4 N_4 - \cdots) - (1-c)^2(\alpha^3 N_3 + \alpha^5 N_5 + \cdots)}{(1-c)^2(1-\alpha^4 M_4 - \alpha^6 M_6 - \cdots) + \alpha(H_1 - \alpha^2 M_3 - \alpha^4 M_5 \cdots)}.$$

An approximate value of α is put into the right-hand side to obtain an approximation of the higher order on the left-hand side. For the initial approximation, take $\alpha = 0$.

c) *Numerical accuracy of the calculations.* The numerical accuracy of our calculation as based upon the final equations given in section 6 are limited by several factors:

i) by neglecting quantities of the orders e^{-P} and $(\alpha R)^{-1}$ in the reduction of the determinantal equations of the boundary-value problems,

ii) by using the inviscid solutions for ϕ_1 and ϕ_2 (error of the order (αR^{-1})),

iii) by the approximations of the rapidly varying solutions ϕ_3 and ϕ_4 as discussed at the end of §6,

iv) by the boundary-layer approximation used in setting up the equation of stability (except in the cases of plane Couette and Poiseuille flows).

Finally, certain numerical approximations have to be used in the actual evaluation of the quantities u and v in equations (11.11). We shall now discuss these factors one by one.

The inaccuracy due to (i) and (ii) is negligible in all the cases considered, because αR is always sufficiently large. In connection with (iii), the situation is more compli-

cated. The first approximation of the asymptotic solution should give an error of the order of $(\alpha R)^{-1/2}$; while the first approximation using Hankel functions should give an error of the order $(\alpha R)^{-1/3}$. It might therefore be thought that the asymptotic method should always give a better approximation. However, this is not the case. For the order of accuracy of the first method is based upon a fixed value of y, while that of the second is based upon a fixed value of η. Thus, if αR may be allowed to become very large while $y-y_0$ remains to be of the order of unity, the first method is definitely better. This is the case with the quantities ϕ_{42} and ϕ'_{42}. With ϕ_{31} and ϕ'_{31}, the situation is different. Here, y_1-y_0 is always small. Except for one branch of the neutral curve for profiles with a flex, y_1-y_0 goes to zero as αR becomes infinite. Because of the smallness of y_1-y_0, the asymptotic solution (which fails to be accurate in the neighborhood of y_0) never gives a good approximation. This is why the other method has to be used in most of the calculations, and we are limited to an accuracy of $(\alpha R)^{-1/3}$. We note that the curvature of the velocity distribution does not come into this approximation. Thus, for better accuracy, a second approximation should be used, the error being then reduced to the order of $(\alpha R)^{-2/3}$. However, since the error in the method used is only a few per cent, and an improvement in accuracy would not alter the general conclusions, it does not seem worth while to improve the accuracy in the light of general interest. Indeed, the inaccuracy due to the other causes (to be discussed) is also of the same order of magnitude. Another support to the method used is that it does agree with the asymptotic method when z is large; there is only a negligible difference (cf. eq. (6.31)).

The effect of the change of the thickness of the boundary layer might be taken to be more serious than a mere numerical inaccuracy. Taylor regarded this as invalidating the existing instability theory of the boundary layer. This question can best be settled experimentally. For the present, we only want to discuss its effect upon our boundary value problem. An approximate estimate of this effect may be obtained by considering the change of the thickness of the boundary layer for one wavelength of the disturbance. This can be easily verified* to be $\pi(1.72)^2/\alpha_1 R_1$. For the lowest value of $\alpha_1 R_1$ involved in the calculations of §13, this is about 6 per cent. Thus, the error is not large. Hence, in the physical interpretation of the results, we need only consider a change of Reynolds number as we pass down stream. One interesting point is the following: as the Reynolds number keeps on increasing, all disturbances finally become stable, if the linear theory holds throughout. Thus, the transition to turbulence depends upon the occurrence of the non-linear effect and hence must depend upon the amount of initial disturbance.

d) *Calculation of* $\phi_{12}^{(0)}$, $\phi_{22}^{(0)}$, *etc.* We shall now discuss the method by which these quantities are evaluated for the calculation of u and v in the equations (5) and (7). A discussion of the accuracy of the present method and of Tollmien's method of evaluating these quantities will also be made.

The original question is to evaluate the integrals $H_m(c)$ and $K_m(c)$ as occurring in (6.24). Various methods are possible for carrying out the calculation, including straightforward numerical integration. The method to be described is an attempt at a simple one. With the transformations (2), we hope to bring out the dominant terms of the series (6.24), and the calculations of u and v according to (7) and (9) are based upon the use of the transformed series (1). We make the following approximations.

* Cf. Goldstein [7], last column of table of p. 157.

i) The imaginary part v is chiefly given by that of the first term, namely, $w_1' c(K_1+1/w_1' c)$; this implies that the imaginary part due to $H_2(c)$, $M_3(c)$, $N_3(c)$, etc. is negligible.

ii) The real part receives also little contribution from those of $H_2(c)$, $M_3(c)$, $N_3(c)$, etc., and hence these need be calculated only approximately.

iii) The series are cut short; terms like N_4, M_4, $\cdots$ are entirely neglected.

Let us proceed to justify these approximations.

The justification of (ii) and (iii) is based upon the following two facts.

a) The quantities in the series involved decrease roughly like $1/m!$, m being the number of integrations involved in defining a certain term.

b) For $\alpha<1$, the terms also decrease as α^m. Thus, the accuracy is not very good for $\alpha>1$, namely for low Reynolds numbers.

But from a consultation of Tables V and VI, and the manner in which the integrals $H_2(c)$, $M_3(c)$, $H_3(c)$, etc., enter (5) and (7), we see that an error of ten per cent in these integrals will cause a negligible error in the final results.

The justification of (i) needs more explanation. For definiteness, let us take $N_3(c)$ as an example. Now,

$$N_3(c) = \int_{y_1}^{y_2} dy(w-c)^{-2} \int_{y_1}^{y} dy(w-c)^2 \int_{y_1}^{y} dy(w-c)^{-2}.$$

This can be expressed as the sum of the following three integrals:

$$N_{31}(c) = K_1(c) \cdot \int_{y_1}^{y_0} dy(w-c)^2 \int_{y}^{y_2} dy(w-c)^{-2},$$

$$N_{32}(c) = \int_{y_1}^{y_2} dy(w-c)^{-2} \int_{y_0}^{y} dy(w-c)^2 \int_{y}^{y_2} dy(w-c)^{-2},$$

$$N_{33}(c) = \int_{y_0}^{y_2} dy(w-c)^{-2} \int_{y_0}^{y} dy(w-c)^2 \int_{y}^{y_2} dy(w-c)^{-2}.$$

The third integral is real, because $y>y_0$. A further transformation of the last integration in N_{31} and N_{32} like

$$\int_{y}^{y_2} dy(w-c)^{-2} = K_1(c) - \int_{y_1}^{y} dy(w-c)^{-2}$$

gives

$$N_{31} = \{K_1(c)\}^2 \int_{y_1}^{y_0} dy(w-c)^2 - K_1(c) \int_{y_1}^{y_0} dy(w-c)^2 \int_{y_1}^{y} dy(w-c)^{-2}$$

$$N_{32} = K_1(c) \int_{y_1}^{y_0} dy(w-c)^{-2} \int_{y_0}^{y} dy(w-c)^2 - \int_{y_1}^{y_0} dy(w-c)^{-2} \int_{y_0}^{y} dy(w-c)^2 \int_{y_1}^{y} dy(w-c)^{-2}.$$

Now, the last integral is real because $y<y_0$. Further, it can be easily verified that

$$\int_{y_1}^{y_0} dy(w-c)^2 \int_{y_1}^{y} dy(w-c)^{-2} = \int_{y_1}^{y_0} dy(w-c)^{-2} \int_{y_0}^{y} dy(w-c)^2.$$

Hence, the only term which can contribute to the imaginary part of $N_3(c)$ is $\{K_1(c)\}^2 \int_{y_1}^{y_0} dy(w-c)^2$. Now, c is usually small so that we may put

$$\int_{y_1}^{y_0} dy(w-c)^2 = \frac{w_1'^2}{3}(y_1 - y_0)^3 = \frac{1}{3}\frac{(w_1' c)^3}{w_1'^4}.$$

Hence,

$$\{K_1(c)\}^2 \int_{y_1}^{y_0} dy(w-c)^2 = \{w_1' cK_1(c)\}^2 \frac{1}{3}\frac{w_1' c}{w_1'^4}.$$

Now we have approximately

$$w_1' cK_1(c) = 1 - vi.$$

Substituting into the above expression, we obtain the imaginary part of $N_3(c)$ as $-2w_1' cv/3w_1'^4$. This will give a contribution of approximately $-(2/3)\{\alpha c(1-c)/w_1'\}^2 v$ to the imaginary part of v. This is negligible, because the factor preceding v is at most of the order of 0.02 in our calculations. Hence, it is justifiable to neglect the contribution of N_3 to v. With the other terms, the approximation is even better; thus, the imaginary part of $H_2(c)$ is of the order of c^3 times that of $K_1(c)$, and that of $M_3(c)$ is of the order of c^6 times that of $K_1(c)$.

Having thus justified the approximations described above, the task is to evaluate $K_1(c)$, $H_1(c)$, $H_2(c)$, $M_3(c)$, and $N_3(c)$ with proper degree of accuracy. For parabolic distribution, these integrals can be evaluated exactly; the approximation (ii) is not necessary. Thus,

$$H_1(c) = A, \tag{11}$$

$$K_1(c) = -\frac{1}{2a^2(1-a^2)} + \frac{A}{2a^3}\left\{\log\frac{1+a}{1-a} + i\pi\right\}, \tag{12}$$

$$H_2(c) = \frac{1}{30}\frac{4a^2-3}{a^2} + \frac{A}{2a^3}\log(1+a) - \frac{2a^2}{15}\log a^2 - \frac{B}{4a^3}\{\log(1-a^2) - i\pi\}, \tag{13}$$

$$M_3(c) = \frac{B^2}{2a^2}K_1 + \frac{8a^2A}{15}\left\{\frac{1}{a+1} + \log\frac{a+1}{a}\right\} + \frac{1}{225}\left\{-\frac{54}{7} + \frac{108}{5}a^2 - \frac{38}{3}a^4 - 64a^6\right\}, \tag{14}$$

$$Rl\, N_3(c) = \frac{1}{24a^2}(1+3a^2) - \frac{(1-a^2)^2}{16a^5}\log\frac{1+a}{1-a} + \frac{1}{16a^6}\left\{\int_0^1 dx\left\{(a^2-x^2)\log\left|\frac{a+x}{a-x}\right|\right\}^2 - B\pi^2\right\}, \tag{15}$$

$$ImN_3(c) = \frac{\pi}{16a^6}\left\{2B\log\frac{1+a}{1-a} + \frac{32a}{15}\log\frac{1+a}{2a} - \frac{2a}{15}(1-a)(2+3a+18a^2+20a^3)\right\}, \tag{16}$$

where

$$a^2 = 1 - c, \qquad A = a^4 - \frac{2a^2}{3} + \frac{1}{5}, \qquad B = A - \frac{8a^5}{15}. \tag{17}$$

These are the equations on which Table V is based, where only the real parts are given. For any other profile, the rule is as follows:

i) Evaluate $K_1(c)$ with as much accuracy as possible. Usually, it is broken up into two parts. Thus,

$$K_1(c) = K_{11}(c) + K_{12}(c); \qquad K_{11}(c) = \int_{y_1}^{y_j} dy(w-c)^{-2},$$

$$K_{12}(c) = \int_{y_j}^{y_2} dy(w-c)^{-2}, \tag{18}$$

where $y_1 < y_j < y_2$. The value of y_j is chosen so that $K_{11}(c)$ can be calculated with sufficient accuracy by developing w as a power series of $(y-y_0)$, while $K_{12}(c)$ can be evaluated by developing the integrand as a power series of c/w.

ii) Evaluate by numerical integration the quantities

$$H_1(0) = \int_{y_1}^{y_2} dyw^2, \tag{19}$$

$$H_1'(0) = -2\int_{y_1}^{y_2} wdy \tag{20}$$

$$H_2(0) = \int_{y_1}^{y_2} w^{-2}dy\int_{y_1}^{y} w^2dy, \tag{21}$$

$$M_3(0) = \int_{y_1}^{y_2} w^2dy\int_{y}^{y_2} w^{-2}dy\int_{y_1}^{y} w^2dy, \tag{22}$$

$$N_3(0) = \int_{y_1}^{y_2} w^{-2}dy\int_{y_1}^{y} w^2dy\int_{y}^{y} w^{-2}dy. \tag{23}$$

iii) The integral $H_1(c)$ is then given by

$$H_1(c) = H_1(0) + H_1'(0)c + c^2. \tag{24}$$

iv) The real part of the integrals $H_2(c)$, $M_3(c)$, $N_3(c)$ are obtained by comparison with the corresponding quantities for parabolic distribution (Table V). For example,

$$M_3(c) - M_3(0) = \left(\frac{w'}{2}\right)^2 \times \text{corresponding quantity for parabolic distribution.} \tag{25}$$

The idea of the last step is essentially to approximate the given profile with a parabolic one.

For the Blasius profile, (with $w_1' = 2$, $y_j - y_1 = 0.4$). We obtain

$$\left.\begin{aligned} K_{11}(c) + \frac{1}{w_1' c} &= -0.5615 - 0.3937c - 1.543c^2 - 1.803c^3 - 1.368c^4 - 5.022c^5 \\ &\quad + \cdots + \frac{9}{8}\left(c^2 + \frac{21}{8}c^5 + \cdots\right)\left(\log\frac{0.8 - c}{c} + i\pi\right), \\ K_{12}(c) &= 0.7080 + 1.3546c + 2.588c^2 + 3.860c^3 + 5.446c^4 + 7.455c^5 \\ &\quad + \cdots, \\ K_1(c) + \frac{1}{w_1' c} &= 0.1465 + 1.2467c + 1.045c^2 + 2.039c^3 + 4.078c^4 + 2.423c^5 \\ &\quad + \cdots + \frac{9}{8}\left(c^2 + \frac{21}{8}c^5 + \cdots\right)\left(\log\frac{0.8 - c}{c} + i\pi\right). \end{aligned}\right\} \tag{26}$$

In evaluating these integrals, we take

$$\left.\begin{aligned} w &= 2(y - y_1) - 3(y - y_1)^4, && 0 \leqq y - y_1 \leqq 0.4, \\ w &= 1 - \{0.9 - (y - y_1)\}^2, && 0.4 < y - y_1 \leqq 0.9, \\ w &= 1 && 0.9 \leqq y - y_1 \leqq 1. \end{aligned}\right\} \tag{27}$$

For the integrals $H_1(0)$ and $H_1'(0)$, we make use of the known values of the displacement thickness and the momentum thickness δ_2.

$$\left.\begin{aligned} \delta_1 &= \frac{1}{6}(1.7208) = 0.28673, \\ \delta_2 &= \frac{1}{12}(1.32824) = 0.11067. \end{aligned}\right\} \tag{28}$$

Thus,

$$H_1(0) = 1 - \delta_1 - \delta_2 = 0.6026, \qquad H_1'(0) = -2(1 - \delta_1) = -1.4265. \tag{29}$$

The values of $H_2(0)$, $M_3(0)$, $N_3(0)$, as evaluated by numerical integration, are given in the first row of Table VI. The rest of the table is constructed by following the procedure described above.

We see that the method of approximation developed above is purely a numerical one, and the calculation can be done without excessive labor. In any case, even if the above method does not give satisfactory results, suitable approximations can always be devised for the evaluation of the necessary integrals. This is the advantage of using Heisenberg's form of the inviscid solutions. In the method used by Tollmien, it is necessary that the *profile* may be approximated by linear and parabolic parts; otherwise, the numerical labor is excessive. It is not clear at once what is the effect of such an approximation on the solutions $\phi(y)$. A more serious criticism of Tollmien's method is the joining of the inviscid solutions at the point of junction of the two approximate profiles. Mathematically speaking, such a junction presents an essential singularity in the coefficients of the differential equation (3.8) or (3.14). Numerically speaking, serious difficulty would be expected when c is equal or even only very near to the velocity of junction, because the inviscid solution fails at the critical layer where $w = c$. Tollmien did not publish how he overcame this difficulty.*

* Tollmien [73], footnote, p. 37.